Superconductivity in layered binary silicides: A density functional theory study

José A. Flores-Livas,[1] Régis Debord,[1] Silvana Botti,[2,1] Alfonso San Miguel,[1] Stéphane Pailhès,[1,3] and Miguel A. L. Marques[1]
[1]*Université de Lyon, FR-69000 Lyon, France and LPMCN, CNRS, UMR 5586, Université Lyon 1, FR-69622 Villeurbanne, France*
[2]*Laboratoire des Solides Irradiés and ETSF, École Polytechnique, CNRS, CEA-DSM, FR-91128 Palaiseau, France*
[3]*Institut Rayonnement Matière de Saclay, Laboratoire Léon Brillouin, CEA-CNRS UMR 12, CE-Saclay, FR-91191 Gif-sur-Yvette, France*
(Received 29 June 2011; revised manuscript received 12 October 2011; published 4 November 2011)

A class of metal disilicides (of the form XSi_2, where X is a divalent metal) crystallizes in the $EuGe_2$ structure, formed by hexagonal corrugated silicon planes intercalated with metal atoms. These compounds are superconducting like other layered superconductors, such as MgB_2. Moreover, their properties can be easily tuned either by external pressure or by negative chemical pressure (i.e., by changing the metal), which makes disilicides an ideal testbed to study superconductivity in layered systems. In view of this, we present an extensive density functional theory study of the electronic and phonon band structures as well as the electron-phonon interaction of metal disilicides. Our results explain the variation of the superconducting transition temperature with pressure and the species of the intercalating atom, and allow us to predict superconductivity for compounds not yet synthesized belonging to this family.

DOI: 10.1103/PhysRevB.84.184503 PACS number(s): 74.70.Ad, 71.15.Mb, 74.20.−z, 74.25.Kc

I. INTRODUCTION

The surprising discovery of record-breaking superconductivity in MgB_2 at 39 K (see Ref. 1) has been a guide for much of the experimental and theoretical research on conventional superconductivity for the past years. Many important results have appeared, and several structures (many of which hypothetical) with very high superconducting transition temperatures (T_c) have been proposed. Examples are Li_xBC ($T_c = 150$ K),[2] carbon clathrates ($T_c = 77$ K),[3] silanes under high pressure ($T_c = 17$ K),[5] or even metallic hydrogen, where T_c was predicted to reach as much as 242 K at extreme pressures of 450 GPa.[6] Lately, we have also witnessed a revived interest in superconductivity of the so-called "covalent metals,"[9] such as boron-doped diamond,[10] intercalated graphite,[11] doped silicon,[12] doped silicon carbide,[13] alkaline-earth silicon clathrates,[14,15] binary silicides,[16,17] ternary silicides,[18] and many others. Note that superconductivity in all these systems is due to the electron-phonon mechanism, hence these materials can be classified as conventional Bardeen-Cooper-Schrieffer (BCS) superconductors.

One of the main characteristics of MgB_2 (and also of other high-T_c superconductors like the cuprates or the iron pnictides) is the reduced dimensionality related to the layered nature. It is therefore not surprising that other layered materials composed of flat plans with sp^2 bonding, such as CaC_6 and YbC_6,[29,30] were extensively studied in the years following the discovery of MgB_2. Another particularly interesting example of 2D-intercalated compounds are metal disilicides (of the form XSi_2, where X is a divalent metal), which can possess either semiconducting or metallic phases.[19,20] Superconductivity was found in such layered structures,[16,19,21] with transition temperatures ranging from the mK to around 15 K.[24] The $EuGe_2$-type XSi_2 disilicides crystallize in an hexagonal honeycomb structure with the metal atoms between the Si plans with an AA stacking. This forms an sp^3 Si network that presents a natural buckling on the Si sheets.[16,19,22] Experimentally, a large range of intercalating metals can be used, namely, alkaline-earth metals (Ca, Sr, Ba) and lanthanides (Eu, La, Ce, Pr, Th, Nd, Gd, Sm, Y, Dy, Yb, Er, Tm, Lu, etc.). More information about these compounds can be found in the excellent reviews on silicon polymorphous and 2D Si-puckered layers by Yamanaka,[24] Imai,[22] and Demchyna.[25]

Few experimental and theoretical works studied superconductivity in metal disilicides. For $CaSi_2$, T_c was found experimentally to increase as a function of pressure, arriving at 14 K.[16,17] This was interpreted as coming from a flattening of the Si planes, resulting from an sp^3-sp^2 phase transition above 16 GPa. The structure with flat Si planes (AlB_2 phase) is not stable at ambient conditions, but can be in principle stabilized through hole doping, which leads to the filling of the π bands, increasing the sp^2 character of silicon.[26,27] More recently, superconductivity was found at 8.9 K in another disilicide, namely, $BaSi_2$. This was achieved through the decrease of the buckling of the Si plane, affecting directly the electron-phonon coupling between the Si out-of-plane phonon and the heavy metal.[28]

It is clear from these two cases that there are two paths to reduce the bucking of the Si planes, and therefore to alter the superconducting transition temperature: (i) by applying positive mechanical pressure or (ii) by intercalation with larger ions (negative chemical pressure). Note that, however, these two paths have an opposite effect on the cell volume: it descreases in (i) but increases in (ii).

It is the aim of this work to give a better understanding of the mechanisms behind the variation of T_c in the disilicides and to provide hints on how superconductivity can be enhanced. For that, we perform density functional theory (DFT) calculations for different intercalating atoms, along the alkali earth column (Mg, Ca, Sr, Ba, Ra). After analyzing the electronic structure, phonon spectrum, and the electron-phonon coupling matrix elements, we correlate these properties to the transition temperatures obtained from McMillan's formula.

The rest of this paper is organized as follows: in Sec. II, we give details on our numerical methodology. The discussion of the structural optimization is given in Sec. III, followed, in Sec. IV, by the results for the electronic structures and Fermi surfaces of disilicides. In Sec. V, we discuss the phonon properties, the electron-phonon coupling, and the

superconducting transition temperatures. Finally, we present our conclusions in Sec. VI.

II. METHODOLOGY

All calculations were performed within DFT using the ABINIT code,[31] in the Perdew, Burke, and Erzernhof (PBE) generalized gradient approximation[32] for the exchange-correlation functional. The electron-ion interaction was described by norm-conserving Troullier-Martins pseudopotentials[33] generated with the same functional. Note that for the elements that compose our compounds and in the pressure range of interest the pseudopotential approximation is reliable. The phonon spectrum and the electron-phonon matrix elements were obtained employing density functional perturbation theory.[34,35] The spectral function $\alpha^2F(\omega)$ was calculated applying the tetrahedron technique for the integration over the Fermi surface. Proper convergence of these quantities was ensured by setting a cutoff energy of 30 Ha, a $16 \times 16 \times 16$ Monkhorst-Pack sampling,[36] and a $4 \times 4 \times 4$ q grid for the phonon wave vectors. Superconducting transition temperatures were calculated through the McMillan approximate solution[40] of the Eliashberg equations.[41]

III. CRYSTAL STRUCTURES

For superconductivity, the most relevant phase of the disilicides compounds is the trigonal (P-3m1,164).[20–22,28] This trigonal structure, depicted in Fig. 1, has metal atoms in the 1a Wyckoff position with reduced coordinates (0,0,0) and Si in the 2d position with reduced coordinates (1/3,2/3,z). The parameter z is extremely important, as it measures the degree of buckling of the silicon planes: the value $z = 1/2$ means completely flat planes.

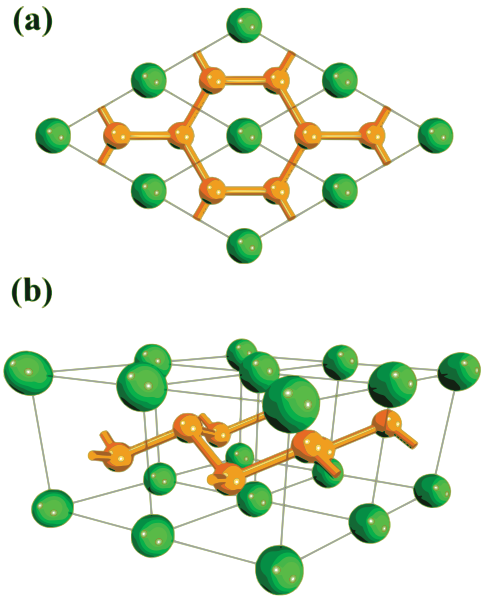

FIG. 1. (Color online) Crystal structure of the disilicides compounds in the trigonal phase (P-3m1,164). The metal atoms are the (green) dark gray larger balls, while the orange (light green) smaller balls represent Si atoms. (a) Projection of the crystal structure onto the ab plane. (b) Layered structure where it is visible the buckling of the Si layer.

TABLE I. Lattice parameters and z values obtained trough geometry optimization for the trigonal phase.

System	a (Å)	c (Å)	Volume (Å^3)	z_{opt}
$MgSi_2$	3.70	4.86	57.6	0.602
$CaSi_2$	3.89	5.01	65.5	0.585
$SrSi_2$	3.96	5.13	69.6	0.573
$BaSi_2$	4.07	5.40	77.4	0.560
$RaSi_2$	4.07	5.09	73.1	0.556

In order to study the effect of chemical pressure, we mainly focused on intercalation with atoms of the column II-A (Mg, Ca, Sr, Ba, Ra). Moreover, the effect of mechanical pressure could be explored for $CaSi_2$ thanks to the availability of experimental data.[16,17,22] Note that we incorporated the hypothetical trigonal structures for $MgSi_2$ and $RaSi_2$ in our set in order to have a better understanding on the variation of T_c along the II-A column.

In Table I, we present the lattice parameters a, c, and z_{opt} that resulted from the geometry optimization. As expected, going down the II-A column the unit cell expands (with the exception of Ra). Moreover, for heavy atoms, we obtain low buckled structures (close to the AlB_2 phase with a $z = 0.5$), while for light atoms the distortion increases leading to a highly buckled structure.

In Fig. 2, we plot the total energy as a function of the internal z parameter at fixed volume. Besides the variation of value of z corresponding to the minimum of the curves, we can also notice that the concavity of the curve increases with increasing atomic number. This concavity is related to the phonon mode that describes the off-plane deformation of the Si layers. One can deduce that, especially for heavy metal atoms, it costs very little energy to change significantly the corrugation of the layers. This was also verified experimentally, as it was possible to produce samples of $BaSi_2$ with different values of

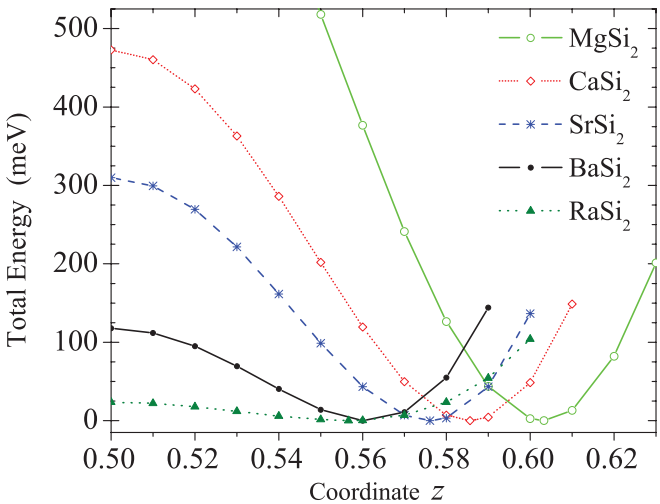

FIG. 2. (Color online) Total energy per XSi_2 unit calculated at 0 GPa for the different disilicides at the lattice parameters a and c given in Table I.

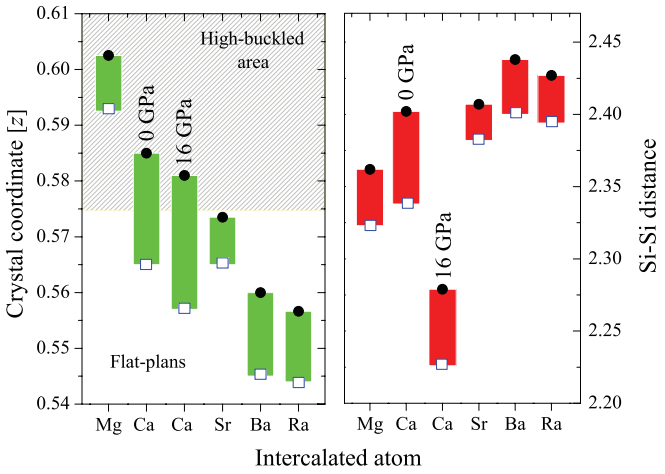

FIG. 3. (Color online) Range of z values (left panel) and Si-Si distances (right panel) for which phonon-frequencies are real for the different systems studied. The black dots represent the fully relaxed z_{opt}/Si-Si distance, while the empty square shows the "tuned z" positions z_{tuned} and the bar indicates the range of stable structures. In the case of $CaSi_2$, we consider two different pressures.

z by changing the synthesis procedure.[28] In the case of $BaSi_2$, it turned out that the structures with values of z closer to 1/2 were more interesting as they exhibited larger values of T_c.[28]

In order to explore the superconducting properties of disilicides, we need to investigate a reasonable range of values of z. To have a working definition for this range, we kept the cell structure fixed at its theoretical minimum, while allowing z to vary in a region that maximizes $N(E_F)$, λ, and T_c, but at the same time assuring the stability of the structures by real phonon frequencies. In our opinion, this recipe generates a reasonable range of z that we can use to discuss the maximum possible transition temperature for each one of the elements of the XSi_2 family studied in this work. We will refer as "tuned z" to the value of $z = z_{tuned}$ that maximizes the density of states at the Fermi level and the superconducting transition temperature, while yielding real phonons. Those values are marked by empty squares in Fig. 3 and given in Table II. Figure 3 summarizes the ranges of z we used in this work (left panel), together with the corresponding variations in the Si-Si distances (right panel). We emphasize that these ranges correspond to variations of the total energy of only a few tens of meV per XSi_2 unit, for example, for Ba it correspond to less than 50 meV. Small atomic numbers (Mg, Ca) favor highly buckled structures, while the $SrSi_2$ system exhibits an intermediate behavior. Finally, the heavier and larger atoms Ba and Ra decrease the corrugation due to the increasing chemical pressure they exert on the Si planes. It is clear that by changing the intercalating atom, i.e., by applying chemical pressure, we can gain control on the corrugation of the hexagonal Si planes.

Another way to modify the buckling of the Si planes is applying an external pressure. As a function of the increasing external pressure, it is intuitive that the buckling of the Si-Si planes should decrease, while the Si–Si distance shortens (as the volume decreases). For the case of $CaSi_2$, for example, z goes from 0.585 at zero pressure to $z = 0.555$ at 16 GPa, while the Si-Si distance reduces from 2.40 Å at zero pressure to 2.21 Å at 16 GPa. It is important to remark that the typical bonding distance in a layered structure is around 2.3–2.7 Å,[24] a range that is respected for all structures studied here at zero pressure. The shortening of the Si-Si distance can be explained from the experimental compressibility of the c axis, larger by a factor of two than the a or b axes.[22] Note that under pressure, as the buckling decreases and the atoms approach, the hybridization of the states increases leading to strong modification of the electronic properties. In the case of the silicides, this leads to an enhancement of T_c.

TABLE II. Summary of properties related to the superconducting state for the metal disilicides studied in this work. The transition temperatures were obtained using McMillan's formula[40] with $\mu^* = 0.1$. The underestimation of T_c can be related to the neglect of multiband effects in McMillan's formula.[44]

System	P (GPa)	z_{tuned}	λ	ω_{log} (K)	T_c (K)
$MgSi_2$	0	0.593	0.79	132	6.0
$CaSi_2$	0	0.565	0.42	190	1.0
$CaSi_2$	16	0.558	1.1	100	8.0
$SrSi_2$	0	0.565	0.50	187	2.2
$BaSi_2$	0	0.545	0.77	156	6.8
$RaSi_2$	0	0.544	0.93	134	8.3

IV. ELECTRONIC STRUCTURE AND FERMI SURFACE

The Fermi surfaces calculated for the different metal intercalations are illustrated in Fig. 4. For the elements of the column II-A, at the tuned z_{tuned} values (see Table II and empty squares in Fig. 3), the Fermi surface is composed of two parts: a large surface centered at the A points and smaller pockets around the M points. For these compounds, the bands around the A point have mostly Si $3p_{xy}$ character and disperse much more in the xy plane than along vertical directions. For the $BaSi_2$ compound, we found that in the limit of structural stability (smallest z), a small third sheet of the Fermi surface composed purely of Si $3s$ states appears in the Brillouin zone.[28] This third sheet can already been seen at zero pressure in $RaSi_2$, due to the negative chemical pressure exerted by this large atom. A surprising fact is the influence of the d states of the metal on the electronic properties, that probably leads to the stability of the trigonal phase. In fact, $MgSi_2$ [see Fig. 4(a)] has a quite different Fermi surface from the other compounds, with small pockets around the H point. This is very likely one of the reasons why neither Mg nor Be form spontaneously a disilicide system.[42]

Finally, in the panels (b) and (c) of Fig. 4 we see the Fermi surface of $CaSi_2$ at zero and 16 GPa. (Our calculations agree with the electronic structure reported previously in Ref. 37.) The increase of the surface with pressure is evident, both around the A point, and in the pockets around the M points and that at 16 GPa cover the whole M-L region. Note that these latter states are composed predominantly by the hybridization of Si $3p_z$ and Ca $4d$ orbitals.

We now turn to the discussion of the electronic density of states at the Fermi level $N(E_F)$, an important quantity for superconductivity. From Fig. 5, we can see that at the relaxed

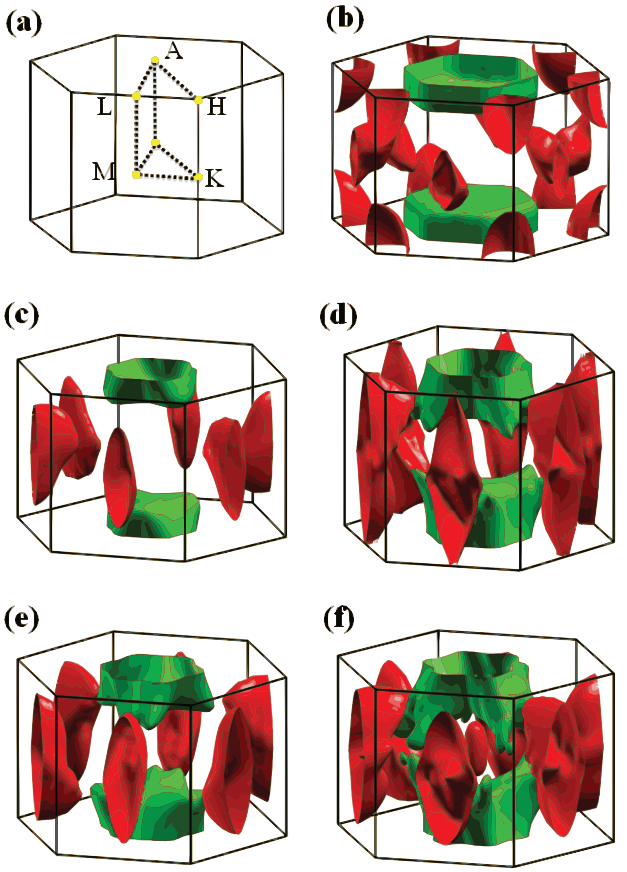

FIG. 4. (Color online) Brillouin zone with high-symmetry points (a) and Fermi surfaces[39] of $MgSi_2$ (b), $CaSi_2$ at the external pressure of 0 GPa (c), $CaSi_2$ at the external pressure of 16 GPa (d), $SrSi_2$ (e), and $RaSi_2$ (f). For $RaSi_2$, note the third sheet appearing at Γ composed purely of Si 3*s* states.

z_{opt} the behavior of $N(E_F)$ with respect to the intercalating atom is not monotonous across the II-A group (green dashed bars), decreasing from Mg to Ca, and then increasing again until Ra. The situation is different if one uses the tuned z_{tuned} (gray solid bars), with $N(E_F)$ now increasing as a function of the atomic number of the metal. For light metals (like Mg), the out-of-plane Si phonon mode is stiff, and therefore there is not much freedom in flattening the planes. This leads to a small difference between $N(E_F)$ at the relaxed and tuned z. On the other hand, for Sr and Ca, one can increase the density of states by 40% and 60%, respectively, by tuning z. This effect is even larger under pressure. For example, at 16 GPa and low buckling, one can increase the density of states at the Fermi level of $CaSi_2$ relatively to its zero pressure and relaxed z_{opt} by as much as 80%. This is explained by the large compressibility on the *c* axis, which leads to an important decrease of volume, and by the softness of the off-plane Si phonon mode that easily allows for large variations of z.

V. PHONONS AND TRANSITION TEMPERATURE

Since there are three atoms per unit cell in the trigonal phase of metal disilicides, the phonon band structures are composed by three acoustic and six (3 × 3-3) optical branches. The

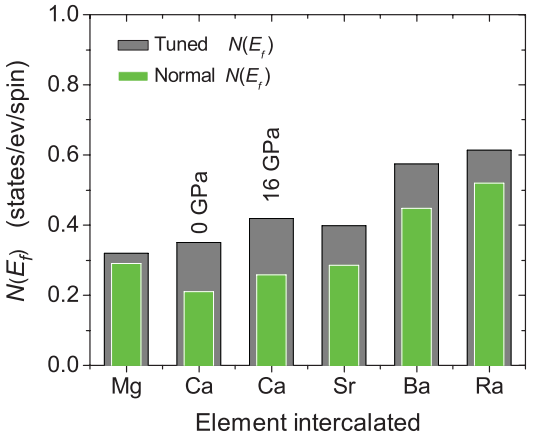

FIG. 5. (Color online) Electronic density of states at the Fermi level $N(E_F)$ for the systems studied in this work. The (green) light gray bars represent calculations at the relaxed geometry $z = z_{opt}$, while the dark gray bars are obtained for the tuned values $z = z_{tuned}$.

mechanical representation for the 1*a* and 2*d* positions in the space group *P*-3*m*1 is $M = A_{1g} + 2A_{2u} + 2E_u + E_g$, where A_{1g} and E_g (double degenerate) are Raman active modes, and A_{2u} and E_u (double degenerate) are infrared active modes. The three higher frequency optical modes involve vibrations of the Si atoms composing the hexagonal planes, while the other, lower-energy three optical modes are out-of-phase vibrations of the Si and metal atoms. These six optical modes, relative to the *P*-3*m*1,164 crystal symmetry of disilicides, are depicted in Fig. 6. The E_g modes describe the in-plane oscillations of Si atoms, while the E_u mode corresponds to the combined out-of-phase movement of the Si and metal atoms in the *xy* plane. On the other hand, the A_{1g} and A_{2u} modes are characterized by the out-of-plane oscillations of, respectively, Si atoms, and out-of-phase Si and metal atoms.

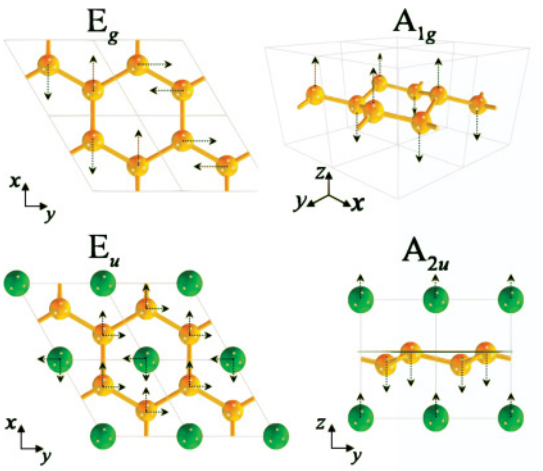

FIG. 6. (Color online) The six optical phonon modes present in the trigonal phase (space group *P*-3*m*1,164) of disilicides. The E_g modes involve the movement of Si atoms in the *xy* plane. The A_{1g} mode represents the out-of-plane motion of the Si atoms. The double degenerate E_u modes are the displacements of individual metal and Si ions in the *xy* plane and the A_{2u} mode is the corresponding out-of-plane displacement.

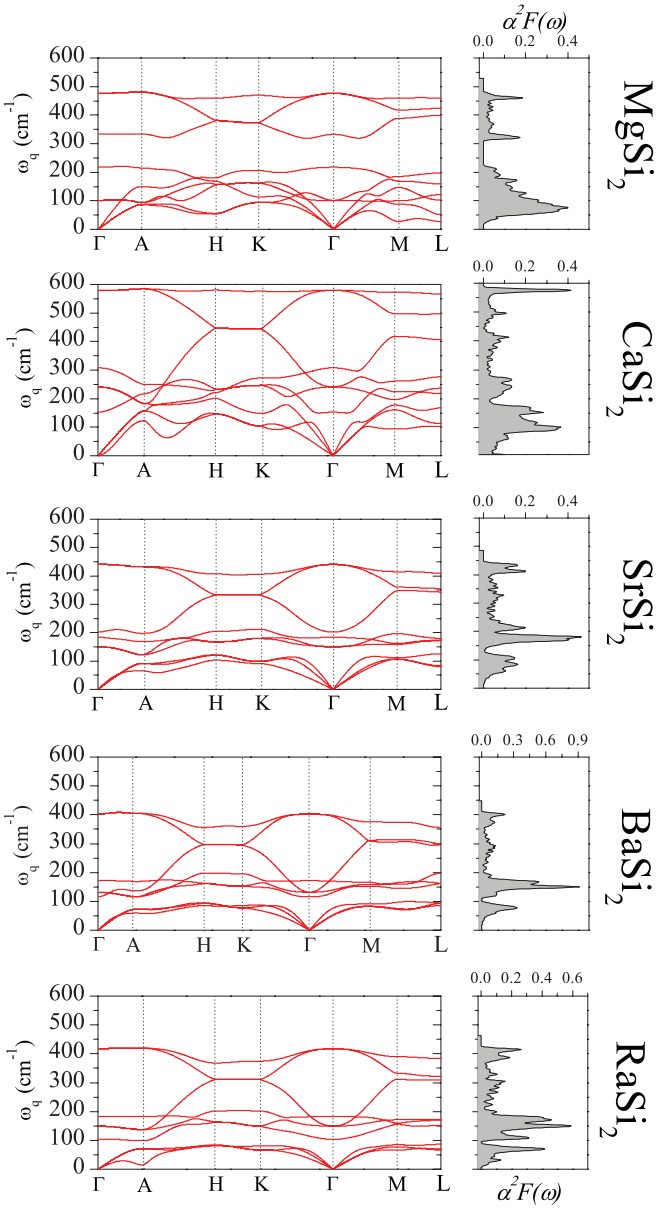

FIG. 7. (Color online) Left panels: Phonon band structure of the disilicides studied in this work. Right panels: Eliashberg spectral function $\alpha^2F(\omega)$ for each structure, calculated for the values of z_{tuned} reported in Table II.

Figure 7 shows the phonon band dispersions for the metal disilicides studied in this work, calculated at the tuned values z_{tuned} of the internal parameter z. In view of the previous experimental and theoretical findings for $BaSi_2$,[28] these calculations should give us access, in principle, to the highest T_c that is possible to attain for each system. There are two important consequences of decreasing the values of z: (i) there is a softening of the phonon modes. In the case of $BaSi_2$, for example, the major effect is on the A_{1g} mode. (ii) As we approach an unstable phase, we generally witness an increase of the electron-phonon interaction.

For each phonon band structure plotted in the left panel of Fig. 7, we also plotted the corresponding spectral function $\alpha^2F(\omega)$, in order to elucidate the origin of the superconducting properties. We remind that, in conventional superconductivity, we should have high-frequency phonon modes strongly coupled to electrons in order to attain large transition temperatures. The related superconducting properties ($\omega_{\log}$, λ, and T_c calculated with McMillan's formula) are presented in Table II. There are two issues concerning to the use of McMillan's formula that should be noticed: (i) this formula requires a value for the parameter μ^* that describes the decrease of the transition temperature due to the breaking of the Cooper pairs interacting through the repulsive Coulomb interaction. In an overwhelming majority of the calculations of T_c this value is semiempirical, or specified through a more or less educated guess. Typical values of μ^* are found between 0.1 and 0.2. For the values of T_c in Table II, we used $\mu^* = 0.1$. (ii) McMillan's formula neglects multiband effects that are known to increase considerably T_c for materials like MgB_2. As the structures studied here have several bands crossing the Fermi level, one can expect that our calculated values for T_c are underestimated. This explains the differences between our calculated transition temperatures and experimental values for $BaSi_2$ and $CaSi_2$. In spite of these two limitations, trends should, however, be correctly described.

As expected, we find in general a softening of the phonon modes for structures with low buckling degree and this effect is enhanced when the mass of the intercalating metal atom increases. The acoustic modes are also found to disperse less for heavier metals. From the $\alpha^2F(\omega)$ plots, we see that all phonon modes couple to electrons, but that the relative weights of each phonon vary with the intercalating metal. For Mg, the acoustic modes softens and are by far the most important, while for Ca, we also see a big peak coming from the high-energy E_g phonon branch, and for Sr, Ba, and Ra, the mixed Si-metal lower-energy optical modes plays an important role.

For the lightest II-A metal studied, Mg, decreasing the buckling does not have a major influence on the A_{1g} out-of-plane vibration that remains (at Γ) close to 340 cm^{-1}, while the E_g frequency at Γ remains at around 470 cm^{-1}. In this case, the phonon modes that cause the structural instability with decreasing z are the acoustic modes that become imaginary at the points M and H of the Brillouin zone. Regarding the spectral function $\alpha^2F(\omega)$ we see that the strongest electron-phonon coupling involves acoustic phonons. Consequently, $\omega_{\log}$ is relatively low, which, combined with the moderate $\lambda = 0.79$, leads to a maximum T_c for this structure of around 6 K.

Ca disilicide has been studied experimentally in Ref. 16 as a function of pressure, and it was found that it can achieve a superconducting transition temperature of 14 K. The samples with highest T_c turned out to be close to the phase transition (at around 16 GPa) between the $EuGe_2$ phase and what was suggested to be the phase of $CaSi_2$ predicted by Kusakabe,[43] which consists in completely flat Si planes ($z = 1/2$) in the AlB_2 structure, leading to a considerable reduction of the volume of the unit cell. However, linear-response calculations of the AlB_2 phase lead to imaginary phonons, and geometry optimization starting from the AlB_2 structure with a slightly broken symmetry yields again a highly buckled structure.[48] These are clear indications that the AlB_2 structure is not stable in the relevant pressure range. On the

other hand, the $EuGe_2$ phase had been previously studied by Nakanishi[38] and Loison.[48] Both works, however, found a theoretical transition temperature much smaller than the maximum experimental value $T_c = 14$ K at 16 GPa.[16] To resolve this issue, we note that, as we know from $BaSi_2$, it is possible to modify z experimentally by applying external pressure, and consequently to enhance superconductivity in $CaSi_2$.

In Fig. 7, we show the phonon dispersion for $CaSi_2$ calculated at the smallest z for which the lattice is theoretically stable. The highest phonon mode (that is strongly coupled to the electronic states) is the E_g in-plane vibration of the Si atoms at around 580 cm^{-1}. Then, at Γ, we find the A_{2u} mode at 240 cm^{-1}, and the A_{1g} mode around 310 cm^{-1}. Note that these values are lower than the ones calculated by Nakanishi[38] and Loison[48] for the trigonal phase of $CaSi_2$. This can be easily explained by the different z used in the calculations, as these previous works used the larger value obtained by geometry minimization within standard DFT.

It is interesting to see how the superconducting transition temperature increases with decreasing value of z. At 16 GPa, and for the highly buckled sample, $z = 0.5876$, $\lambda = 0.3$, and $T_c = 0.1$ K in agreement with the previous calculations.[38] Decreasing z to 0.57 leads to $\omega_{log} = 220$ K and to a slight increase of $\lambda = 0.44$ and $T_c = 1.5$ K. As one reaches $z = 0.56$, there is a sudden increase of the electron-phonon coupling constant to $\lambda = 0.90$ with a $T_c = 5.85$ K. Finally, just before the structure instability indicated by the presence of imaginary phonon frequencies, we obtain for $z = 0.557$ the values of $\lambda = 1.1$, $\omega_{log} = 100$ K, and $T_c = 8$ K. This number is of the same order of magnitude of the maximum experimental $T_c = 14$ K found for $CaSi_2$. The slight underestimation can, moreover, be attributed to the neglect of multiband effects in the McMillan's formula used.

We can now see that the large experimental values of T_c for $CaSi_2$ can be explained without resorting to exotic superconducting mechanisms. Furthermore, the presence of samples with different values of z, can justify, in the same way as for $BaSi_2$,[28] the dispersion of values of T_c found experimentally.

From panel (b) of Fig. 7, we can see that for $CaSi_2$ the phonon modes that contribute more to $\alpha^2F(\omega)$ and therefore to λ are the two E_g modes and the acoustic modes. We should note that, in this case, the acoustic Ca modes become imaginary at low values of z, and therefore are responsible for driving the system to instability.

For the case of heavier intercalated atoms (Sr, Ba, and Ra), we find that the phonon dispersions show very similar structures, the main difference being the energy of the eigenmodes. The Eliashberg spectral functions reveal two main peaks contributing to superconductivity: the first, due to the acoustic modes, less sensitive to changes in z, and the second peak, due to the coupling of electrons with the A_{1g} mode, which moves to lower frequencies for smaller values of z. Descending the II-A column we can also see how the decrease of z induced by the chemical pressure (i.e., by increasing the size of the intercalating atom) leads to an increase of the electron-phonon coupling constants and of the superconducting transition temperature. In fact, the Sr compound has the lowest value of λ with 0.50, leading to $T_c = 2.2$ K, followed by Ba with $\lambda = 0.77$ and $T_c = 6.8$ K. Finally, Ra leads to the highest values $\lambda = 0.93$ and $T_c = 8.3$ K. In conclusion, the order of T_c from the lowest to the highest is Sr, Mg, Ba, Ca, and Ra. Note that, recently, experimental x-ray diffraction measurements of $BaSi_2$ confirmed the variation of T_c as a function of buckling as predicted by *ab initio* calculations.[28] For these heavy intercalating metals, the lattice instability related to the flattening of the hexagonal Si layers comes through the acoustic metal branch that becomes imaginary for small values of z.

It is interesting to consider the relationship between superconductivity trends in the XSi_2 family and silicon clathrates having the same guest atoms (Ca, Sr, Ba). Both families are intercalated silicon structures, but they exhibit different structural constraints. In fact, there is no analogous to the buckling tuning parameter of XSi_2 in silicon clathrates, which on the other hand possess various intercalation sites. If we consider the simplest and more studied case of the type-I clathrate structure X_8Si_{46} with only two intercalation sites, it has been found that the McMillan approximation holds, with T_c essentially controlled by the density of states at the Fermi level.[49,51] This leads to a stronger dependence of T_c on the nature of the guest atom[50] as there is no additional structural tuning parameter.

VI. CONCLUSIONS

In this paper, we studied several compounds belonging to the family of metal disilicides, namely, $MgSi_2$, $CaSi_2$, $SrSi_2$, $BaSi_2$, and $RaSi_2$. We calculated using *ab initio* density functional theory the electronic properties, phonon dispersions, electron-phonon coupling, and superconducting transition temperatures. All these quantities were obtained as a function of the internal coordinate z, an important parameter that measures the buckling of the hexagonal Si planes in the structure. Our results show that it is possible to increase the density of electronic states at the Fermi surface in two different ways, either by reducing the buckling of the Si planes by means of external pressure or by intercalating heavier atoms between the Si sheets. The phonon modes show, as expected, a softening with increasing atomic number of the metal, and the largest electron-phonon coupling comes normally from the acoustic and lowest-lying optical modes. The calculated electron-phonon coupling constants allow to explain superconductivity in $CaSi_2$ and $BaSi_2$, without the need of invoking exotic superconducting mechanisms. Furthermore, the experimental dispersion of values of T_c can be easily explained by the presence of samples with different values of z.

ACKNOWLEDGMENTS

J.A.F.L. acknowledges the CONACyT, Mexico. S.B. acknowledges support from EU's 7th Framework Programme (e-I3 contract ETSF n.211956) and M.A.L.M. from the French ANR (ANR-08-CEXC8-008-01). Calculations were performed at GENCI (project x2011096017).

[1] J. Nagamatsu, N. Nakagawa, T. Muranaka, Y. Zenitani, and J. Akimitsu, Nature (London) **410**, 63 (2001).
[2] H. Rosner, A. Kitaigorodsky, and W. E. Pickett, Phys. Rev. Lett. **88**, 127001 (2002).
[3] D. Connétable, V. Timoshevskii, B. Masenelli, J. Beille, J. Marcus, B. Barbara, A. M. Saitta, G.-M. Rignanese, P. Mélinon, S. Yamanaka, and X. Blase, Phys. Rev. Lett. **91**, 247001 (2003).
[4] N. W. Ashcroft, Phys. Rev. Lett. **21**, 1748 (1968).
[5] M. I. Eremets, I. A. Trojan, S. A. Medvedev, J. S. Tse, and Y. Yao, Science **319**, 5869 (2008).
[6] C. Bersier, A. Floris, P. Cudazzo, G. Profeta, A. Sanna, F. Bernardini, M. Monni, S. Pittalis, S. Sharma, H. Glawe, A. Continenza, S. Massidda, and E. K. U. Gross, J. Phys. Condens. Matter **21**, 164209 (2009).
[7] M. Lüders, M. A. L. Marques, N. N. Lathiotakis, A. Floris, G. Profeta, L. Fast, A. Continenza, S. Massidda, and E. K. U. Gross, Phys. Rev. B **72**, 024545 (2005).
[8] M. A. L. Marques, M. Lüders, N. N. Lathiotakis, G. Profeta, A. Floris, L. Fast, A. Continenza, E. K. U. Gross, and S. Massidda, Phys. Rev. B **72**, 024546 (2005).
[9] X. Blase, E. Bustarret, C. Chapelier, T. Klein, and C. Marcena, Nat. Mater. **8**, 375 (2009).
[10] E. A. Ekimov, V. A. Sidorov, E. D. Bauer, N. N. Mel'nik, N. J. Curro, J. D. Thompson, and S. M. Stishov, Nature (London) **428**, 542 (2004).
[11] N. Emery, C. Hérold, M. dAstuto, V. Garcia, Ch. Bellin, J. F. Marêché, P. Lagrange, and G. Loupias, Phys. Rev. Lett. **95**, 087003 (2005).
[12] E. Bustarret, C. Marcenat, P. Achatz, J. Kaĉmarĉik, F. Lévy, A. Huxley, L. Ortéga, E. Bourgeois, X. Blase, D. Débarre, and J. Boulmer, Nature (London) **444**, 465 (2006).
[13] Z. Ren, J. Kato, T. Muranaka, J. Akimitsu, M. Kriener, and Y. Maeno, J. Phys. Soc. Jpn. **76**, 103710 (2007).
[14] H. Kawaji, Hiro-omi Horie, S. Yamanaka, and M. Ishikawa, Phys. Rev. Lett. **74**, 1427 (1995).
[15] K. Tanigaki, T. Shimizu, K. M. Itoh, J. Teraoka, Y. Moritomo, and S. Yamanaka, Nat. Mater. **2**, 653 (2003).
[16] S. Sanfilippo, H. Elsinger, M. Núñez-Regueiro, O. Laborde, S. LeFloch, M. Affronte, G. L. Olcese, and A. Palenzona, Phys. Rev. B **61**, R3800 (2000).
[17] P. Bordet, M. Affronte, S. Sanfilippo, M. Núñez-Regueiro, O. Laborde, G. L. Olcese, A. Palenzona, S. LeFloch, D. Levi, and M. Hanfland, Phys. Rev. B **62**, 11392 (2000).
[18] R. Heid, K.-P. Bohnen, B. Renker, P. Adelmann, T. Wolf, D. Ernst, and H. Schober, J. Low Temp. Phys. **147**, 375 (2007).
[19] J. Evers, J. Solid State Chem. **32**, 77 (1980).
[20] M. Imai and T. Hirano, J. Alloys Compd. **224**, 111 (1995).
[21] M. Imai, K. Hirata, and T. Hirano, Physica C **245**, 12 (1995).
[22] M. Imai and T. Kikegawa, Chem. Mater. **15**, 2543 (2003).
[23] K.-P. Bohnen, R. Heid, and B. Renker, Phys. Rev. Lett. **86**, 5771 (2001).
[24] S. Yamanaka, Dalton Trans. **39**, 1901 (2010).
[25] R. Demchyna, S. Leoni, H. Rosner, and U. Schwarz, Z. Kristallogr. **221**, 420 (2006).
[26] G. Satta, G. Profeta, F. Bernardini, A. Continenza, and S. Massidda, Phys. Rev. B **64**, 104507 (2001).
[27] C. Bersier, A. Floris, A. Sanna, G. Profeta, A. Continenza, E. K. U. Gross, and S. Massidda, Phys. Rev. B **79**, 104503 (2009), and references therein.
[28] J. A. Flores-Livas, R. Debord, S. Botti, A. San Miguel, M. A. L. Marques, and S. Pailhès, Phys. Rev. Lett. **106**, 087002 (2011).
[29] M. Calandra and F. Mauri, Phys. Rev. Lett. **95**, 237002 (2005).
[30] L. Boeri, G. B. Bachelet, M. Giantomassi, and O. K. Andersen, Phys. Rev. B **76**, 064510 (2007).
[31] X. Gonze, G.-M. Rignanese, M. Verstraete, J.-M. Beuken, Y. Pouillon, R. Caracas, F. Jollet, M. Torrent, G. Zerah, M. Mikami, Ph. Ghosez, M. Veithen, V. Olevano, L. Reining, R. Godby, G. Onida, D. Hamann, and D. C. Allan, Kristallogr. **220**, 558 (2005).
[32] J. P. Perdew, K. Burke, and M. Ernzerhof, Phys. Rev. Lett. **77**, 3865 (1996).
[33] M. Fuchs and M. Scheffler, Comput. Phys. Commun. **119**, 67 (1999).
[34] S. Y. Savrasov and D. Y. Savrasov, Phys. Rev. B **54**, 16487 (1996).
[35] S. Y. Savrasov, Phys. Rev B **54**, 16470 (1996).
[36] H. J. Monkhorst and J. D. Pack, Phys. Rev. B **13**, 5188 (1976).
[37] S. Fahy and D. R. Hamann, Phys. Rev. B **41**, 7587 (1990).
[38] A. Nakanishi, T. Ishikawa, H. Nagara, and K. Kusakabe, J. Physics: Conferences Series **121**, 052010 (2008).
[39] The Fermi surfaces were ploted using XCRYSDEN. A. Kokalj, Comput. Mater. Sci. **28**, 155 (2003). Code available from [http://www.xcrysden.org/].
[40] W. L. McMillian, Phys. Rev. **167**, 331 (1968).
[41] G. M. Eliashberg, Zh. Eksp. Teor. Fiz. **38**, 966 (1960) [Sov. Phys. JETP **11**, 696 (1960)].
[42] T. B. Massalski, *Binary Alloys Phase Diagram*, edited by H. Okamoto and ASM International, 2nd ed. (ASM International, Materials Park, OH, 1990).
[43] K. Kusakabe, Y. Tateyama, T. Ogitsu, and S. Tsuneyumi, J. Phys. Condens. Matter **10**, 11561 (1998).
[44] A. Y. Liu, I. I. Mazin, and J. Kortus, Phys. Rev. Lett. **87**, 087005 (2001).
[45] J. Evers, J. Solid State Chem. **20**, 173 (1977).
[46] J. Sangster, J. Phase Equilib. Diffus. **27**, 192 (2006).
[47] The values of V found theoretically are slight shifted compared to the experimental values V_{exp}. This usually leads to softer phonons.
[48] C. Loison and H. Rosner, Solid State Commun. **150**, 2076 (2010).
[49] P. Toulemonde, Ch. Adessi, X. Blase, A. San Miguel, and J. L. Tholence, Phys. Rev. B **71**, 094504 (2005).
[50] P. Toulemonde, A. San Miguel, A. Merlen, R. Viennois, S. Le Floch, Ch. Adessi, X. Blase, and J. L. Tholence, J. Phys. Chem. Solids **67**, 1117 (2006).
[51] Y. Noat, T. Cren, P. Toulemonde, A. San Miguel, F. Debontridder, V. Dubost, and D. Roditchev, Phys. Rev. B **81**, 104522 (2010).